Available online at www.sciencedirect.com
SCIENCE DIRECT®
Journal of Food Engineering 69 (2005) 281–290
JOURNAL OF FOOD ENGINEERING
www.elsevier.com/locate/jfoodeng

Simulation of stirred yoghurt processing in plate heat exchangers

Carla S. Fernandes [a,b], Ricardo Dias [b], J.M. Nóbrega [a], Isabel M. Afonso [c,d], Luis F. Melo [d], João M. Maia [a,*]

[a] Departamento de Engenharia de Polímeros, IPC—Institute for Polymers and Composites, Universidade do Minho, 4800-058 Guimarães, Portugal
[b] Escola Superior de Tecnologia e de Gestão, Instituto Politécnico de Bragança, Campus de Santa Apolónia, 5301-854 Bragança, Portugal
[c] Escola Superior Agrária de Ponte de Lima, Instituto Politécnico de Viana do Castelo, Refóios, 4990-706 Ponte de Lima, Portugal
[d] Faculdade de Engenharia, Laboratório de Engenharia de Processos, Ambiente e Energia - LEPAE, Universidade do Porto, Rua Dr. Roberto Frias, s/n 4200-465 Porto, Portugal

Received 19 February 2004; accepted 6 August 2004

Abstract

In the present work, simulations of stirred yoghurt processing in a plate heat exchanger were performed using computational fluid dynamics (CFD) calculations and the results compared with experimental data, showing a very good agreement.

A Herschel–Bulkley model for the viscosity and an Arrhenius-type term for the temperature dependence were used to model the thermo-rheological behaviour of yoghurt. The heat exchanger used in this study operates in a parallel arrangement, thus simplifying the problem to the construction of a single complete 3D channel.

After analysis of the velocity field and fanning friction factors, laminar flow was observed for all the operating conditions used and relations are proposed for the present heat exchanger between fanning factors and Reynolds number and between mean shear rate and mean velocity of yoghurt.

Keywords: Yoghurt; Plate heat exchanger; Flow and thermal distribution; Computational fluid dynamics

1. Introduction

Stirred yoghurt is a non-Newtonian fluid, obtained by promoting the growth of *Streptococcus salivarius* subsp. *thermophilus* and *Lactobacillus delbrueckii* subsp. *bulgaricus* in milk at a temperature between 40 °C and 43 °C until a desired acidity level is reached. These bacteria are responsible by the production of lactic acid from milk lactose. When the desired acidity is reached, yoghurt must be quickly cooled to a temperature around 20 °C in order to stop lactic fermentation. After cooling, yoghurt is packed and stored at a temperature between 2 °C and 5 °C (Staff, 1998; Tamine & Robinson, 1988).

The rheology of stirred yoghurt has been studied by several authors (Afonso, Hes, Maia, & Melo, 2003; Afonso & Maia, 1999; Benezech & Maingonnat, 1993; Rohm & Kovac, 1994, 1995; Rönnegård & Dejmek, 1993); for example, Afonso and Maia (1999) studied the influence of temperature on viscosity and identified two regions with different temperature dependencies, observing a more pronounced dependency above 25 °C.

Recently, Afonso et al. (2003) studied the rheological behaviour of yoghurt during the cooling processing and identified two regions with distinct shear rate dependency on viscosity. For shear stress lower than 6.7 Pa the studied yoghurt exhibited Bingham viscoplastic behaviour and for shear stress higher than 6.7 Pa a shear-thinning behaviour.

Plate heat exchangers are commonly used on the processing of foods. Due to several advantages of this

* Corresponding author. Fax: +351 53 510 339.
E-mail address: jmaia@dep.uminho.pt (J.M. Maia).

0260-8774/$ - see front matter © 2004 Elsevier Ltd. All rights reserved.
doi:10.1016/j.jfoodeng.2004.08.018

Nomenclature

List of symbols

a	constant (-)
A	area (m^2)
A_p	projected area (m^2)
b	body forces vector (N)
b	distance between plates (m)
C_p	specific heat of fluids ($Jkg^{-1}K^{-1}$)
D_e	equivalent hydraulic diameter (m)
E	activation energy ($Jmol^{-1}$)
f	fanning friction factor (-)
F	correction factor (-)
h	heat supply or strength of an internal heat source (W)
I	unit tensor (-)
K, K_1, K_2	consistency index ($Pa.s^n$)
L	effective length (m)
L_T	length (m)
M	mass flow rate per channel (kgs^{-1})
m_v	volumetric flow rate per channel (m^3s^{-1})
M_v	total volumetric flow rate (m^3s^{-1})
n	flow behaviour index (-)
N_c	number of channels (-)
N_p	total number of plates (-)
p_c	wavelength of corrugation (m)
q	heat flux vector (Wm^{-2})
q	heat flux (Wm^{-2})
r	cylindrical coordinate (m)
R	ideal gas constant ($Jmol^{-1}K^{-1}$)
Re	Reynolds number (-)
T	total stress tensor (Pa)
T	absolute temperature (K)
u	velocity vector (ms^{-1})
u	mean velocity (ms^{-1})
U	overall heat transfer coefficient ($Wm^{-2}K^{-1}$)
v	local velocity (ms^{-1})
w	effective width (m)
w_T	width (m)
x, y, z	spatial coordinates (m)

Greek Symbols

β	Corrugation angle (°)
ΔP	pressure drop (Pa)
ΔT_{ml}	mean logarithmic temperature difference (K)
ϕ	area enlargement factor (-)
$\dot{\gamma}$	shear rate (s^{-1})
$\bar{\dot{\gamma}}$	mean shear rate (s^{-1})
$\dot{\gamma}_{max}$	maximum shear rate (s^{-1})
η_{app}	apparent viscosity (Pa.s)
λ_p	thermal conductivity of the plates ($WK^{-1}m^{-1}$)
ρ	fluid density (kgm^{-3})
σ	extra stress tensor (Pa)
σ	shear stress (Pa)
σ_0	yield stress (Pa)
υ	parameter (-)
ξ	geometrical parameter (-)

Subscripts

in	inlet
out	outlet
PHE	plate heat exchanger
pp	infinite parallel plates
wat	cooling water
yog	yoghurt

type of heat exchangers, like their high efficiency, ease of maintenance and cleaning and flexibility on account of modular design (Reppich, 1999), previous experimental and modelling works have been focused on the optimization of their project and design, namely, arrangements and configurations (Bassiouny & Martin, 1984; Gut & Pinto, 2003a, 2003b), pressure drop and fanning factors (Antonini, François, & Shuai, 1987; Leuliet, Maigonnat, & Lalande, 1987, 1990) and influence of corrugation angle on flow behaviour (Ciofalo, Stasiek, & Collins, 1996; Mehrabian & Poulter, 2000; Stasiek, Collins, Ciofalo, & Chew, 1996). However, most of the above studies were performed for Newtonian fluids and, out of those that did not the majority restricted the analysis to isothermal flows. The aim of present work is to overcome some of the shortcomings above and study the thermal and hydrodynamics characteristics of yoghurt processing in plate heat exchangers using a non-isothermal and non-Newtonian analysis.

2. Problem description

Usually, cooling treatment of stirred yoghurt is carried out in plate heat exchangers since these equipments are suitable for liquid–liquid heat transfer duties that require uniform and rapid cooling or heating. In this operation, two mechanisms of heat transfer occur: conduction, in the plates, and convection inside the channels.

So, in order to simulate the non-isothermal flow of stirred yoghurt in a plate heat exchanger three problems were solved simultaneously: one of non-isothermal flow inside the channel and two of heat conduction in the plates.

2.1. Governing equations

Fourier's law, Eq. (1), governs the heat conduction in the plates,

$$\boldsymbol{q} = -\lambda_p \nabla T, \tag{1}$$

where $\boldsymbol{q}$ is the heat flux vector, λ_p the thermal conductivity of the plates and T the absolute temperature.

The equations required to describe a laminar flow are known as the Navier–Stokes equations. This set of equations comprises the conservation equations for mass, linear momentum and energy (Chandrasekharaiah & Debnath, 1994).

The simulations were carried out considering stationary flow of incompressible fluid, so equations above assume, respectively, the form:

$$\mathrm{div}(\boldsymbol{u}) = 0, \tag{2}$$

$$\mathrm{div}\boldsymbol{T} + \rho\boldsymbol{b} - \rho\mathrm{div}(\boldsymbol{uu}) = 0, \tag{3}$$

$$\boldsymbol{T} \cdot \nabla\boldsymbol{u} + \rho h - \mathrm{div}\boldsymbol{q} = 0, \tag{4}$$

where $\boldsymbol{u}$ is the velocity vector, $\boldsymbol{T}$ the total stress tensor and h refers to the heat supply or strength of an internal heater.

Eqs. (2)–(4) represent five transport equations with thirteen unknown variables: u_i, T_{ij}, q_i (i,j = 1,2,3) and h.

2.2. Constitutive modelling

To describe the rheological behaviour of stirred yoghurt during cooling treatment in the present plate heat exchanger, experimental and modelling results from Afonso et al. (2003), that found the behaviour to be of the Herschel–Bulkley-type, were used:

$$\sigma = \sigma_0 + K_1\dot{\gamma} \quad \text{for } \sigma < 6.7\text{Pa}, \tag{5a}$$

$$\sigma = K_2\dot{\gamma}^n \quad \text{for } \sigma \geqslant 6.7\text{Pa}, \tag{5b}$$

σ_0 being the yield stress, K_1 and K_2 consistency indices and n the flow behaviour index.

Under the operating conditions in the plate heat exchanger, the fluid has a predominant shear-thinning behaviour, since, as will be shown below, in all conditions $\sigma \geqslant 6.7$ Pa. Thus, the constitutive equation was based in Eq. (5b), the influence of temperature being introduced by a term of the Arrhenius type:

$$\eta_{app}(T) \propto e^{E/RT}, \tag{6}$$

where E is the activation energy and R the ideal gas constant. In Eq. (5b), $K_2 = 3.65\,\text{Pa.s}^{0.42}$, $n = 0.42$ and $E = 94785\ \text{Jmol}^{-1}$.

3. Numerical simulation

The set of governing and constitutive equations presented in Section 2 was solved using the commercial finite element method package POLYFLOW. Numerical simulations were performed using a Dell Workstation PWS530 with 1 GB of RAM and were divided in three steps:

- construction of geometrical domain and mesh generation;
- establishment of boundary conditions and properties of the system;
- numerical resolution of the finite element problem.

Simulations were performed for 15 flow rates of yoghurt, correspondent to the operating conditions and fluid properties from Afonso et al. (2003).

3.1. Geometrical domain and mesh generation

The simulated heat exchanger was a Pacetti RS 22. The plates had the geometrical characteristics shown in Table 1 and were constructed considering an effective length, L, and width, w, represented in Fig. 1(a) (Kakaç & Liu, 2002). The corrugations were described by a sine curve (Mehrabian & Poulter, 2000):

$$y(x) = \frac{b}{2}\sin\left(\frac{2\pi}{p_c}\left(x - \frac{p_c}{4}\right)\right) + \frac{b}{2}, \tag{7}$$

where b is the distance between plates and p_c the wavelength of corrugation (Fig. 1(b)).

Since the plate heat exchanger had a parallel arrangement (Afonso et al., 2003) and admitting a uniform distribution of the total flow rate in the various channels, the flow simulations of yoghurt were carried out in a single channel. Additionally, uniform flow was considered inside each channel and, for this reason, a symmetry axis was established (Fig. 1) simplifying the geometrical domain to half of a channel (Fig. 2).

Although the computational domain was highly complex due to the multiple contractions and expansions along the channel, it was found that a mesh constituted by tetrahedral, hexahedral, prismatic and pyramidal elements was adequate (Fig. 3).

A grid independency test was also performed. Simulations were carried out using meshes with different

Table 1
Main geometrical characteristics of the herringbone plates

Material	Stainless steel AISI 316
Plate model	RS 22
Area, A (m^2)	0.015
Length, L_T (m)	0.265
Width, w_T (m)	0.102
Effective length, L (m)	0.19
Effective width, w (m)	0.072
Area enlargement factor, $\phi(-)$	1.096
Corrugation angle, β	30°
Wavelength of corrugation, $p_c \times 10^3$ (m)	10
Distance between plates, $b \times 10^3$ (m)	2.6
Thickness, $x_p \times 10^3$ (m)	0.5
Thermal conductivity, λ_p ($Wm^{-1}K^{-1}$)	16.3

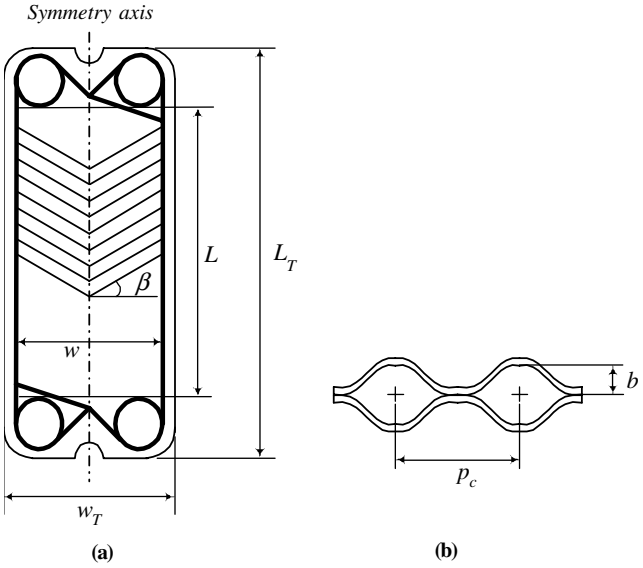

Fig. 1. (a) Schematic representation of a chevron plate; (b) Corrugations dimensions.

Fig. 2. Geometrical domain.

distance between nodes: 2, 1.5, 1.2 and 1 mm. To evaluate the influence of the mesh in the obtained results, mean velocities were compared. Values obtained with the two finest grids were similar (deviation of 0.02%) and distant from the obtained with the others. Since computational time was higher when using the 1 mm mesh, calculations on present work were made using the mesh with 1.2 mm of node distance. The used mesh has 173 634 elements and 37 237 nodes.

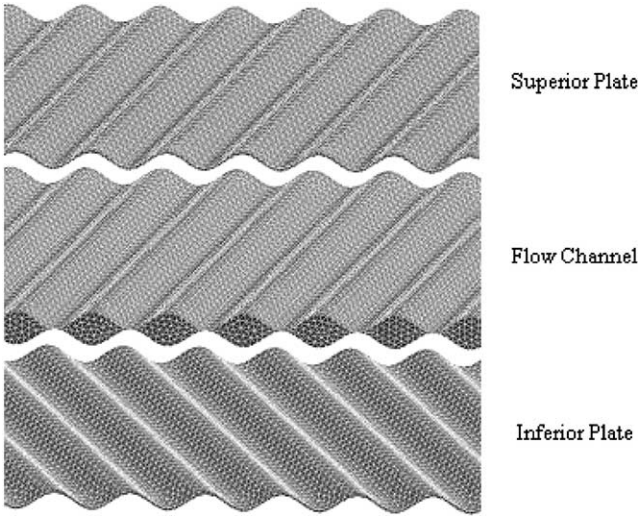

Fig. 3. Part of the used mesh.

3.2. Boundary conditions

Since experimental data was available (Afonso et al., 2003), boundary conditions were determined based on this data, taking into account that the plate heat exchanger studied in this work operates with parallel arrangement and in counterflow.

Thus, the yoghurt volumetric flow rate per channel, m_v, was given by:

$$m_v = \frac{M_v}{N_c}, \tag{8}$$

where M_v is the total volumetric flow rate of yoghurt and N_c the number of channels,

$$N_c = \frac{N_p - 1}{2}, \tag{9}$$

with N_p the total number of plates.

Since the geometrical domain represents half of a channel, the volumetric flow rate used was half of the value determined by Eq. (8).

Inlet temperature of yoghurt was established according to the experimental data and two alternative types of thermal boundary conditions were imposed along the plates: a variable heat flux and a constant heat flux.

The profile of heat flux along the plates, $q(x)$, was deduced in the case of counterflow as (Appendix A):

$$q(x) = UF\left(T_{yog_{in}} - T_{wat_{out}}\right) \times \exp\left[2ULF\phi x\left(\frac{1}{M_{wat}C_{p_{wat}}} - \frac{1}{M_{yog}C_{p_{yog}}}\right)\right], \tag{10}$$

where x is the dimension on the main flow direction ($0 \leqslant x \leqslant L$), U is the overall heat transfer coefficient, F the correction factor M the mass flow rates per channel, C_p the specific heat and ϕ the area enlargement factor (Kakaç & Liu, 2002), which is given by:

$$\phi = \frac{\text{Effective Area}}{\text{Projected Area}}. \tag{11}$$

In this equation, the effective area is that specified by the manufacturer and the projected area, A_p, is just the product of the effective width, w, and the effective length, L:

$$A_p = wL. \tag{12}$$

Values of U, M and C_p were imposed for each simulation according to experimental data and F was assumed to be 0.942 (Raju & Bansal, 1986).

The constant or average heat flux in the plates was calculated resorting to an energy balance to the yoghurt and the total area of the plates:

$$q = \frac{M_{\mathrm{yog}} C_{\mathrm{p_{yog}}} \left(T_{\mathrm{yog_{in}}} - T_{\mathrm{yog_{out}}}\right)}{2A}. \quad (13)$$

Although Eq. (10) is closer to reality, in the absence of the necessary experimental data, simplified boundary conditions such as Eq. (13), which is a particular case of Eq. (10) when $M_{\mathrm{wat}} C_{\mathrm{p_{wat}}}$ equals $M_{\mathrm{yog}} C_{\mathrm{p_{yog}}}$, must be used instead.

Unfortunately, POLYFLOW only allows a constant or linear profile of heat flux as boundary condition and, thus, Eq. (10) had to be written in a linear form, Fig. 4:

$$q(x) = q(0) + \frac{q(L) - q(0)}{L} x. \quad (14)$$

The average deviation between Eqs. (10) and (14) was 1.39% for the 15 simulations performed.

In all the simulations slip at the wall and heat losses to the surroundings were assumed to be non-existent.

3.3. Numerical resolution

Resolution of Navier–Stokes equations is a non-linear problem, so it was necessary to use an iterative method to solve them. In order to evaluate the convergence of this process, a test based on relative error (in velocity and temperature fields) was made (Polyflow, 2000), and the convergence test value was set to 10^{-4}.

To solve initial problems of convergence introduced by the slow value of n and high value of E, the numerical resolution had to be divided in two steps.

First, the problem was solved without the influence of temperature, that is, the constitutive equation was reduced to the power-law,

$$\eta_{\mathrm{app}}(\dot{\gamma}) = K_2 \dot{\gamma}^{n-1}, \quad (15)$$

and Picard's iteration method was used to solve the initial value problem associated with it.

Subsequently, the results were used as an initial condition and the non-isothermal problem was solved. During this phase, an evolution process had to be implemented. In this process, a sequence of new problems was generated and the activation energy value raised from one problem to another until the real value was achieved ($E = 94\,785$ Jmol^{-1}).

4. Results and discussion

Numerical results concerning the difference between inlet and outlet yoghurt temperature were compared with experimental data and a mean deviation of 6.9% and 7.3% for the simulations with variable and constant heat flux, respectively, was observed.

Similar outlet temperatures were obtained using variable and constant heat flux but the former induced a quicker initial cooling of the yoghurt, as shown in Fig. 5 (this was constructed calculating an average temperature of fluid in planes of equation x = const).

Analyzing the local behaviour of the temperature in the channel, Fig. 6 and Fig. 7, it can be seen that near the contact points between the plates the fluid is subjected to greater cooling, which can be explained by the lower velocities in these regions, as observed in Fig. 8.

Fig. 8, in conjunction with Fig. 9, allows the flow to be characterized as 3D, and the inexistence of turbulence confirms that it is laminar in the present operating conditions, as predicted by Afonso et al. (2003).

Another way to evaluate the flow regime consists in the determination of fanning friction factor, f. The obtained relation between this factor and Reynolds number, Re, was a typical relation for laminar flows (Kakaç & Liu, 2002):

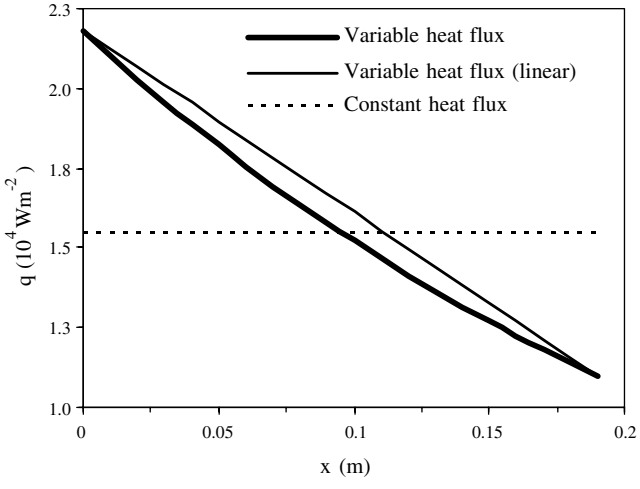

Fig. 4. Thermal boundary condition for Re = 0.46.

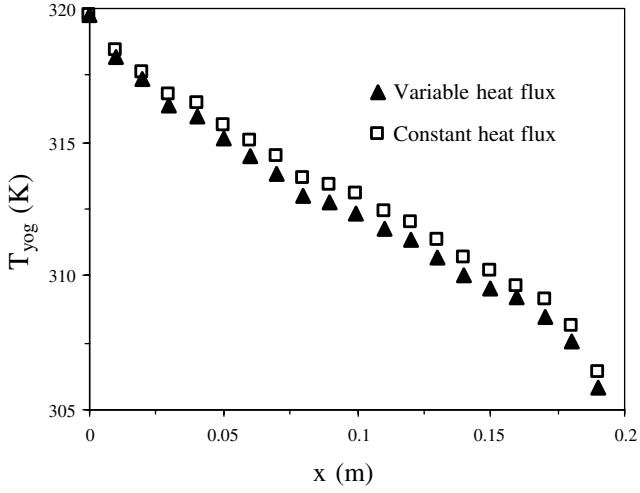

Fig. 5. Temperature profile for Re = 2.7.

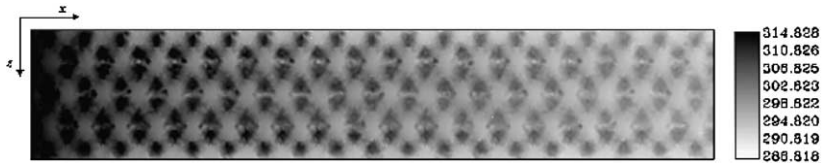

Fig. 6. Temperature distribution on plane of contact points ($y = 0$) for Re = 2.7.

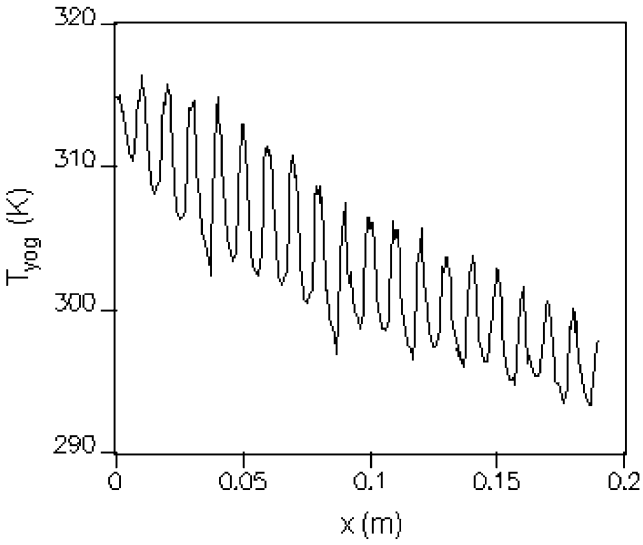

Fig. 7. Temperature profile on plane of contact points ($y = 0$) and $z = 0.025$ for Re = 2.7.

$$f = \frac{a}{Re}, \tag{16}$$

where a is a constant and f and Re are given by:

$$f = \frac{\Delta P D_e}{2L\rho u^2}, \tag{17}$$

$$Re = \frac{\rho u D_e}{\eta_{app}}. \tag{18}$$

In above equations ΔP is the pressure drop, η_{app} is the average viscosity of yoghurt and were both calculated resorting to POLYFLOW. u is the average velocity of yoghurt, D_e is the hydraulic diameter and are given by:

$$u = \frac{m_v}{wb}, \tag{19}$$

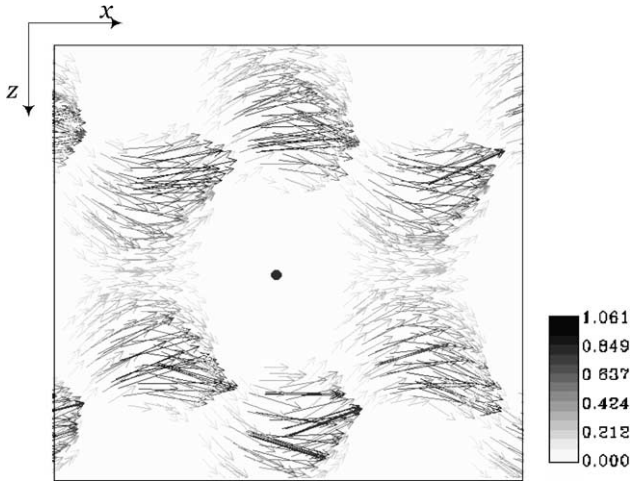

Fig. 8. Velocity vectors around a contact point (●) in the plane of contact points ($y = 0$) for Re = 12.3.

$$D_e = 2b. \tag{20}$$

Yoghurt density, ρ, used in Eqs. (17) and (18) was obtained experimentally (Afonso et al., 2003) and ranged from 1042 to 1071 $kg\,m^{-3}$.

To the current heat exchanger and present operating conditions ($0.31 \leqslant Re \leqslant 12.3$), Eq. (16) takes the form, Fig. 10:

$$f = 50.367\ Re^{-1.0038} \text{ with } R^2 = 0.9979, \tag{21}$$

$$f = 52.606\ Re^{-1.0098} \text{ with } R^2 = 0.9988, \tag{22}$$

for variable and constant heat flux, respectively.

The values for the constant a in Eq. (16) are disperse in the literature (Kakaç & Liu, 2002; Leuliet et al., 1987, 1990; Mehrabian & Poulter, 2000), with studies with non-Newtonian fluids being very scanty, but seems to decrease with corrugation angle, β (Kakaç & Liu, 2002; Mehrabian & Poulter, 2000).

Fig. 9. Velocity vectors in the plane $z = 0.015$ for Re = 12.3.

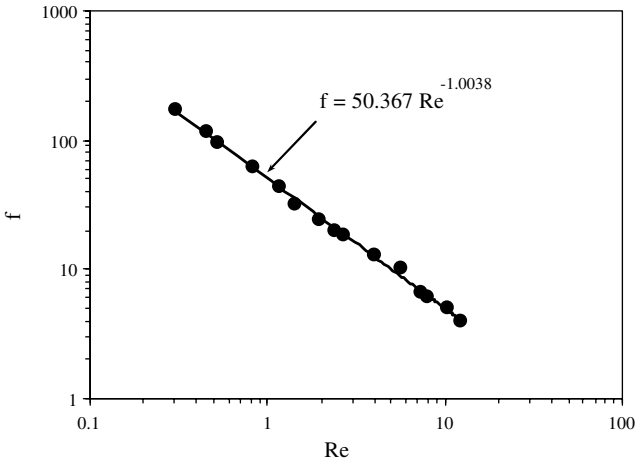

Fig. 10. Fanning friction factor for simulations with variable heat flux.

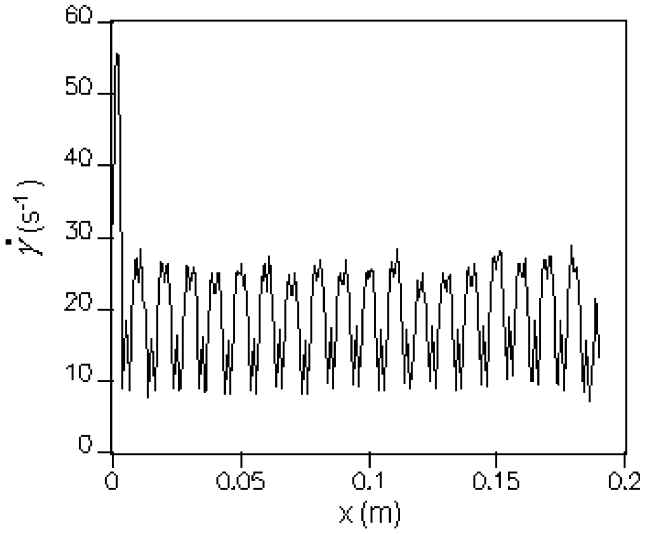

Fig. 11. Shear rate profile in the plane of contact points ($y = 0$) and $z = 0.09$ for Re = 0.31.

For Newtonian fluids and laminar regime, typical values for constant a are well established and, in the particular case of *chevron* plates, it is known that a decreases with the corrugation angle and varies between 24 and 50 for $\beta \geqslant 65°$ and $\beta \leqslant 30°$, respectively (Kakaç & Liu, 2002), which agrees well with our results, i.e., Eqs. (21) and (22). For non-Newtonian fluids, on the other hand the few existent studies in laminar regime are in isothermal conditions (Leuliet et al., 1987, 1990) and with different plates of the present work, namely, *chevron* plates with $\beta = 30°$.

The magnitude of the shear rate inside the heat exchanger is determinant on the consistency of packed yoghurt. Figs. 11 and 12 shows the local behaviour of shear rate, $\dot{\gamma}$, and it can be observed that $\dot{\gamma}$ exhibits a sinusoidal variation along the channel with constant amplitude, with the lowest values being achieved in stagnation zones, that is, around the contact points.

Delplace and Leuliet (1995), proposed for the calculation of maximum shear rate, $\dot{\gamma}_{max}$, in a generic duct:

$$\dot{\gamma}_{max} = \xi\left(\frac{\upsilon n + 1}{(\upsilon + 1)n}\right)\frac{u}{D_e}. \tag{23}$$

For infinite parallel plates the coefficients ξ and υ assume the value of 12 and 2, respectively. In complex ducts the analytical deduction of the referred coefficients is not possible and the authors propose for their determination:

$$\xi = \frac{f}{2}Re, \tag{24}$$

$$\upsilon = \frac{24}{\xi}. \tag{25}$$

Taking into account Eqs. (21), (24) and (25), it is possible to determine $\xi = 25.184$ and $\upsilon = 0.953$ for the present heat exchanger. Fig. 13 shows the very good agreement (maximum deviation of 4%) between the maximum shear rates obtained by CFD calculations

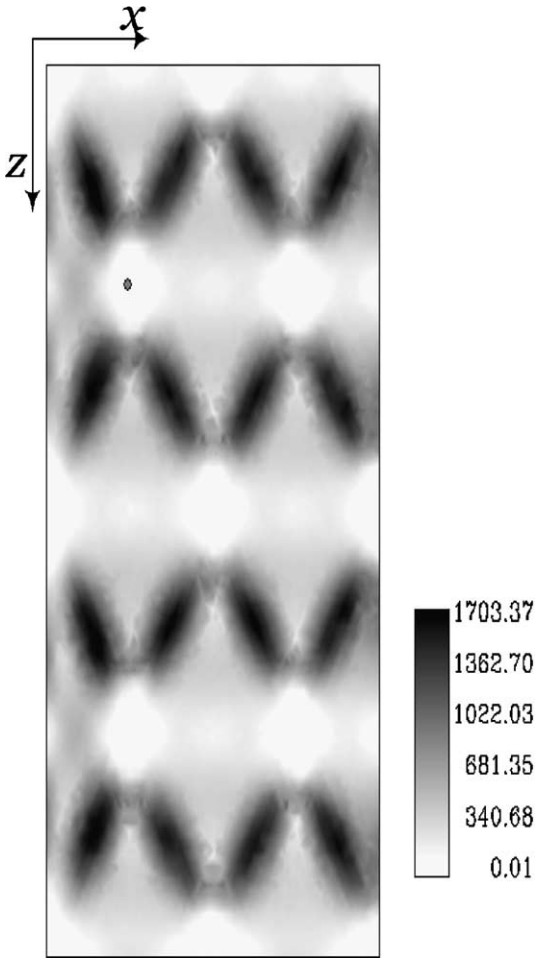

Fig. 12. Shear rate in the plane of contact points ($y = 0$) for Re = 12.3. (●) contact point.

and the predicted by Eq. (23). This shows that the model developed by Delplace and Leuliet (1995) under laminar

and isothermal conditions is largely applicable to a non-isothermal flow with Reynolds number defined by Eq. (18). From Fig. 13 it is also possible to confirm that the maximum shear rates observed in plate heat exchanger are higher than the obtained for infinite parallel plates with the same equivalent hydraulic diameter.

In what regards average shear rates and for infinite parallel plates, $\bar{\dot{\gamma}}_{pp}$ is given by (see Appendix B):

$$\bar{\dot{\gamma}}_{pp} = 4\frac{2n+1}{n+1}\frac{u}{D_e}. \tag{26}$$

For the parallel plates, the relation between mean, $\bar{\dot{\gamma}}_{pp}$, and maximum shear rate can be easily deduced. Taking in account that the maximum shear rate for infinite parallel plates is given by Eq. (23) with $\xi = 12$ and $\upsilon = 2$, the relation is:

$$\bar{\dot{\gamma}}_{pp} = \frac{n}{n+1}\dot{\gamma}_{max}. \tag{27}$$

Then, by resorting to Eq. (25) and considering that Eq. (27) is valid for the plate heat exchanger, the average shear rate in the plate heat exchanger comes as:

$$\bar{\dot{\gamma}}_{PHE} = \xi\frac{\upsilon n+1}{(\upsilon+1)(n+1)}\frac{u}{D_e}. \tag{28}$$

Fig. 14 shows the good agreement (maximum deviation of 7%) between mean shear rate obtained by CFD calculations and predicted by Eq. (28), but further experiments and simulations are needed to try to generalise these results. Again, and as expected, the mean shear rates in the plate heat exchanger are higher than that ones obtained in infinite parallel plates.

Apparent viscosity follows the sinusoidal behaviour of shear rate, but the amplitude of the curve increases along the channel, Fig. 15, which is explained by the decrease in temperature. The apparent shear stress, σ, was estimated for all the simulations and the average values

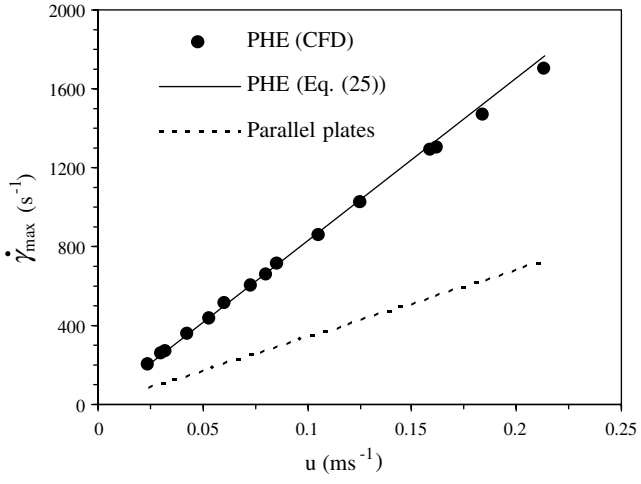

Fig. 13. Maximum shear rate for plate heat exchanger (PHE) and infinite parallel plates.

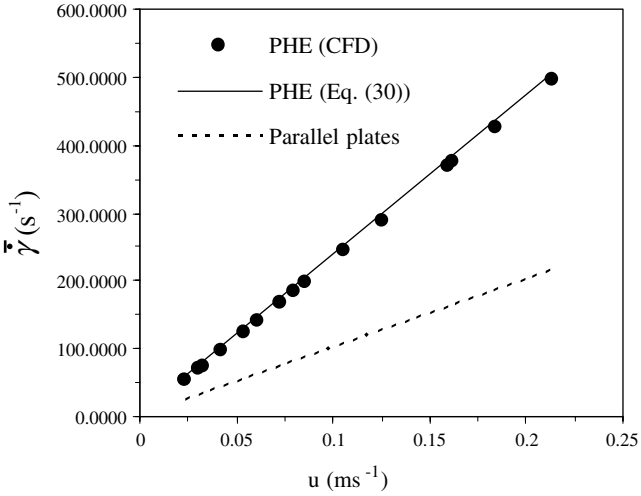

Fig. 14. Mean shear rate for plate heat exchanger (PHE) and infinite parallel plates.

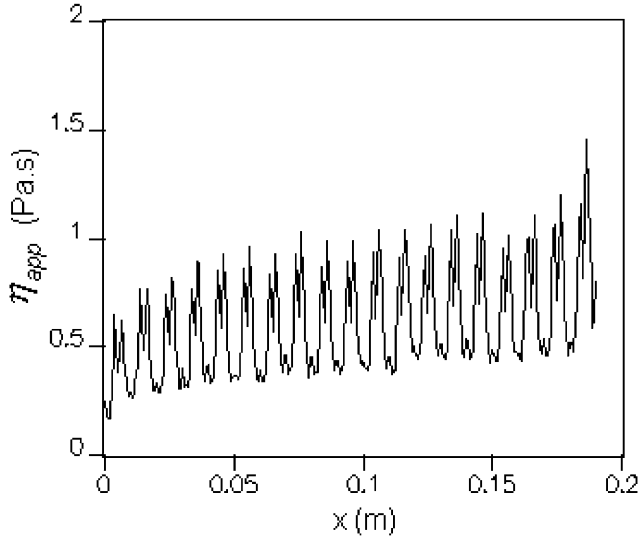

Fig. 15. Apparent viscosity profile in the plane of contact points ($y = 0$) and $z = 0.09$ for Re = 0.31.

ranged from 20 Pa to 46 Pa, which are clearly higher than 6.7 Pa, i.e., the apparent yield stress for the present yoghurt.

5. Conclusions

The objectives of this work were to study the flow behaviour of stirred yoghurt in the complex channels of a plate heat exchanger using a fully non-isothermal, non-Newtonian setting and to construct a tool for project and design of plate heat exchangers for non-Newtonian fluids.

Simulations have been performed considering a 3D geometry that intends to represent a complete channel

of a plate heat exchanger. Resorting to the results of velocities field and the calculated fanning factors it was possible to conclude that a laminar flow occurs in the present operation conditions; the existence of corrugations in the plates confers to temperature, velocity, viscosity and shear rate a sinusoidal behaviour in the main flow direction.

In order to describe the heat exchange between yoghurt and cooling water, two different boundary conditions were imposed: variable and constant heat flux. The latter is a particular case of the former and can be useful when experimental data is not available.

Predictions of CFD calculations were compared to experimental data, and these were found to be in very good agreement.

Appendix A. Derivation of heat flux expression, Eq. (10)

The heat transferred from yoghurt to cooling water in an element of a plate with area dA (Fig. 16) is given by:

$$\mathrm{d}Q = UdAF\left(T_{\mathrm{yog}}(x) - T_{\mathrm{wat}}(x)\right), \tag{A.1}$$

with

$$\mathrm{d}A = L\phi\mathrm{d}x. \tag{A.2}$$

From Eqs. (A.2) and (A.1),

$$\frac{\mathrm{d}Q}{\mathrm{d}x} = UL\phi F\left(T_{\mathrm{yog}}(x) - T_{\mathrm{wat}}(x)\right). \tag{A.3}$$

From fluids energy balances and having in mind that heat exchanger operates in counterflow, it's possible to obtain a math expression for $T_{\mathrm{wat}}(x)$:

$$T_{\mathrm{wat}}(x) = T_{\mathrm{wat_{out}}} - \frac{M_{\mathrm{yog}}C_{\mathrm{p_{yog}}}}{M_{\mathrm{wat}}C_{\mathrm{p_{wat}}}}\left(T_{\mathrm{yog_{in}}} - T_{\mathrm{yog}}(x)\right). \tag{A.4}$$

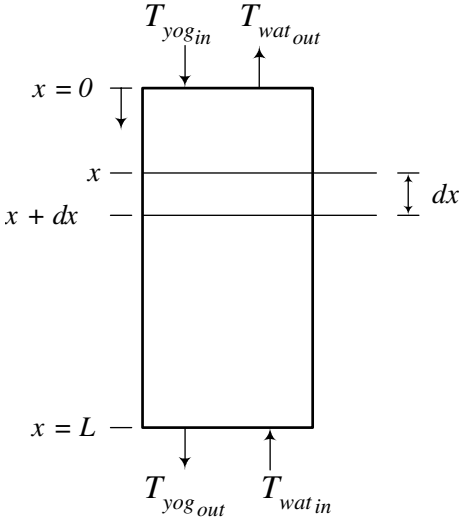

Fig. 16. Schematic representation of an infinitesimal element of a plate.

Thus, Eq. (A.3) can be written as follows:

$$\frac{\mathrm{d}Q}{\mathrm{d}x} = UL\phi F\left[\left(1 - \frac{M_{\mathrm{yog}}C_{\mathrm{p_{yog}}}}{M_{\mathrm{wat}}C_{\mathrm{p_{wat}}}}\right)T_{\mathrm{yog}}(x) - T_{\mathrm{wat_{out}}} + \frac{M_{\mathrm{yog}}C_{\mathrm{p_{yog}}}}{M_{\mathrm{wat}}C_{\mathrm{p_{wat}}}}T_{\mathrm{yog_{in}}}\right], \tag{A.5}$$

and, by other side,

$$\frac{\mathrm{d}Q}{\mathrm{d}x} = -\frac{\mathrm{d}}{\mathrm{d}x}\left(\frac{M_{\mathrm{yog}}}{2}C_{\mathrm{p_{yog}}}T_{\mathrm{yog}}(x)\right). \tag{A.6}$$

So, from equations above, after integration between $x = 0$ and a $x = x$ an expression for $T_{\mathrm{yog}}(x)$ is obtained:

$$T_{\mathrm{yog}}(x) = \frac{1}{1-C}\left\{T_{\mathrm{wat_{out}}} - CT_{\mathrm{yog_{in}}} + \exp\left[-2\frac{UL\phi F}{M_{\mathrm{yog}}C_{\mathrm{p_{yog}}}}(1-C)x\right]\left(T_{\mathrm{yog_{in}}} - T_{\mathrm{wat_{out}}}\right)\right\}. \tag{A.7}$$

where $C = \frac{M_{\mathrm{yog}}C_{\mathrm{Pyog}}}{M_{\mathrm{wat}}C_{\mathrm{Pwat}}}$.

By Eqs. (A.3), (A.2) and (A.7) it can be written the math expression for the heat flux along the plate, $q(x)$:

$$q(x) = \frac{\mathrm{d}Q}{\mathrm{d}A}(x) = UF\left(T_{\mathrm{yog_{in}}} - T_{\mathrm{wat_{out}}}\right) \times \exp\left[2UFL\phi\left(\frac{1}{M_{\mathrm{wat}}C_{\mathrm{p_{wat}}}} - \frac{1}{M_{\mathrm{yog}}C_{\mathrm{p_{yog}}}}\right)x\right]. \tag{A.8}$$

Appendix B. Derivation of mean shear rate expression for infinite parallel plates, Eq. (26)

Force balance in the element represented in Fig. 17 takes the form:

$$2l\sigma = 2y\Delta P \Longleftrightarrow \sigma = \frac{\Delta P y}{l}. \tag{B.1}$$

and for power-law fluid, Eq. (B.1) can be written as:

$$-K\left(\frac{\mathrm{d}v}{\mathrm{d}y}\right)^n = \frac{\Delta P y}{l} \Longleftrightarrow -\mathrm{d}v = \left(\frac{\Delta P}{lK}\right)^{\frac{1}{n}}\sqrt[n]{y}\mathrm{d}y. \tag{B.2}$$

Integrating Eq. (B.2) between $y = y$ and $y = b/2$, having in mind that for laminar regime $v = 0$ in $y = b/2$:

$$v(y) = \left(\frac{\Delta P}{lK}\right)^{\frac{1}{n}}\frac{n}{n+1}\left[\left(\frac{b}{2}\right)^{\frac{n+1}{n}} - y^{\frac{n+1}{n}}\right]. \tag{B.3}$$

Flow rate in two blades with dy thickness is given by:

$$\mathrm{d}M_{\mathrm{v}} = v(y)2\mathrm{d}y. \tag{B.4}$$

Thus, math expression for total flow rate between plates is obtained integrating Eq. (B.4) between $y = 0$ and $y = b/2$ and assumes the form:

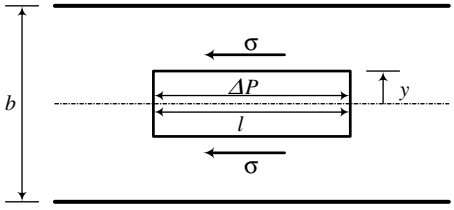

Fig. 17. Schematic representation of infinite parallel plates.

$$M_v = \left(\frac{\Delta P}{lK}\right)^{\frac{1}{n}} \frac{2n}{2n+1}\left(\frac{b}{2}\right)^{\frac{2n+1}{n}}. \quad \text{(B.5)}$$

Consequently, mean velocity can be obtained by:

$$u = \frac{M_v}{b} = \left(\frac{\Delta P}{lK}\right)^{\frac{1}{n}} \frac{n}{2n+1}\left(\frac{b}{2}\right)^{\frac{n+1}{n}}. \quad \text{(B.6)}$$

From Eq. (B.3) maximum velocity is achieved for $y = 0$ and is value is given by:

$$v_{max} = \left(\frac{\Delta P}{lK}\right)^{\frac{1}{n}} \frac{n}{n+1}\left(\frac{b}{2}\right)^{\frac{n+1}{n}}. \quad \text{(B.7)}$$

Dividing Eq. (B.7) by Eq. (B.6) a relation between mean and maximum velocities is obtained:

$$v_{max} = u\frac{2n+1}{n+1}. \quad \text{(B.8)}$$

From Eqs. (B.3), (B.7) and (B.8), math expression is obtained for local velocity:

$$v(y) = u\frac{2n+1}{n+1}\left[1 - \left(\frac{y}{b/2}\right)^{\frac{n+1}{n}}\right]. \quad \text{(B.9)}$$

So, local shear rate is given by:

$$\dot{\gamma}(y) = u\frac{2n+1}{n}\left(\frac{2}{b}\right)^{\frac{n+1}{n}\sqrt{y}}. \quad \text{(B.10)}$$

Consequently, the mean value of shear rate for parallel plates can be mathematically expressed as:

$$\bar{\dot{\gamma}}_{pp} = \frac{\int_0^{b/2}\dot{\gamma}(y)2dy}{\int_0^{b/2}2dy} = 2\frac{2n+1}{n+1}\left(\frac{1}{b}\right)u. \quad \text{(B.11)}$$

Since the infinite parallel plates have an equivalent hydraulic diameter $2b$, Eq. (B.11) can be written as:

$$\bar{\dot{\gamma}}_{pp} = 4\frac{2n+1}{n+1}\frac{u}{D_e}. \quad \text{(B.12)}$$

References

Afonso, I. M., Hes, L., Maia, J. M., & Melo, L. F. (2003). Heat transfer and rheology of stirred yoghurt during cooling in plate heat exchangers. *Journal of Food Engineering, 57*, 179–187.

Afonso, I. M., & Maia, J. M. (1999). Rheological monitoring of structure evolution and development in stirred yoghurt. *Journal of Food Engineering, 42*, 183–190.

Antonini, G., François, O., & Shuai, X. S. (1987). Corrélations transfert/facteur de frottement por le chauffage/refroidissement d'un fluide visqueux à forte dépendance thermorhéologique en écoulement de conduite en régime laminaire. *Revue Générale de Thermique, 308–309*, 427–431.

Bassiouny, M. K., & Martin, H. (1984). Flow distribution and pressure drop in plate heat exchangers—I. *Chemical Engineering Science, 39*(4), 693–700.

Benezech, T., & Maingonnat, J. F. (1993). Flow properties of stirred yoghurt: structural parameter approach in describing time dependency. *Journal of Textures Studies, 24*, 455–473.

Chandrasekharaiah, D. S., & Debnath, L. (1994). *Continuum mechanics*. London: Academic Press (pp. 325–362).

Ciofalo, M., Stasiek, J., & Collins, M. W. (1996). Investigation of flow and heat transfer in corrugated passages – II. Numerical simulation. *International Journal of Heat and Mass Transfer, 39*, 165–192.

Delplace, F., & Leuliet, J. C. (1995). Generalized Reynolds number for the flow of power law fluids in cylindrical ducts of arbitrary cross-section. *The Chemical Engineering Journal, 56*, 33–37.

Gut, J. A. W., & Pinto, J. M. (2003a). Modeling of plate heat exchangers with generalized configurations. *International Journal of Heat and Mass Transfer, 46*, 2571–2585.

Gut, J. A. W., & Pinto, J. M. (2003b). Selecting optimal configurations for multisection plate heat exchangers in pasteurization processes. *Industrial and Engineering Chemistry Research, 42*, 6112–6124.

Kakaç, S., & Liu, H. (2002). *Heat Exchangers Selection, Rating, and Thermal Design* (second ed.). Boca Raton: CRC Press, pp. 131–136, 373–412.

Leuliet, J. C., Maigonnat, J. F., & Lalande, M. (1987). Etude de la perte de charge dans de échangeurs de chaleur à plaques traitant des produits non-newtoniens. *Revue Générale de Thermique, 308-309*, 445–450.

Leuliet, J. C., Maigonnat, J. F., & Lalande, M. (1990). Écoulement et transferts de chaleur dans les échangeurs à plaques traitant des produits visqueux newtoniens et pseudoplastiques. *The Canadian Journal of Chemical Engineering, 68*, 220–229.

Mehrabian, M. A., & Poulter, R. (2000). Hydrodynamics and thermal characteristics of corrugated channels: computacional approach. *Applied Mathematical Modelling, 24*, 343–364.

Polyflow user's guide, ver. 3.8 (2000). Fluent Inc., Centerra Resource Park 10 Cavendish Court, Belgium.

Raju, K. S. N., & Bansal, J. C. (1986). Design of plate heat exchangers. In J. W. Palen (Ed.), *Heat exchanger sourceboo* (pp. 563–582). Berlin: Springer-Verlag.

Reppich, M. (1999). Use of high performance plate heat exchangers in chemical and process industries. *International Journal of Thermal Science, 38*, 999–1008.

Rohm, H., & Kovac, A. (1994). Effects of starter cultures on linear viscoelastic and physical properties of yoghurt gels. *Journal of Structure Studies, 25*, 311–329.

Rohm, H., & Kovac, A. (1995). Effects of starter cultures on small deformation rheology of stirred yoghurt. *Lebensmittel-Wissens chaft und-Technologie-Food Science and Technology, 28*, 319–322.

Rönnegård, E., & Dejmek, P. (1993). Development of breakdown of structure in yoghurt studied by oscillatory rheological measurements. *Le Lait, 73*, 371–379.

Staff, M. C. (1998). Cultured milk and fresh cheeses. In R. Early (Ed.), *The technology of dairy products* (pp. 123–144). London: Blackie Academic & Professional.

Stasiek, J., Collins, M. W., Ciofalo, M., & Chew, P. E. (1996). Investigation of flow and heat transfer in corrugated passages – I. Experimental results. *International Journal of Heat and Mass Transfer, 39*, 149–164.

Tamine, A. Y., & Robinson, R. K. (1988). Fermented milks and their future trends. Part II. Technical aspects (review). *Journal of Dairy Research, 55*, 281–307.